Title Page

Charge-Assisted Halogen Bonding in Bromo- and Iodophenylpyridinium Chlorides

Christopher J. Kassl, Dale C. Swenson, and F. Christopher Pigge[*]

Department of Chemistry, University of Iowa, Iowa City, IA, 52242

ABSTRACT: Ten *N*-halophenylpyridinium salts (halogen = Br or I) with chloride (and in one case iodide) counterions have been prepared and structurally characterized in order to examine the degree of solid state halogen bonding exhibited in these systems. *N*-Halophenylpyridinium salts are easily synthesized from existing pyridines, and the cationic pyridinium group is expected to increase the halogen bond donor ability of attached halophenyl moieties. Halide anions functioning as halogen bond acceptors facilitate formation of charge-assisted halogen bonds. All five substrates featuring iodophenyl or diiodophenyl substituents displayed the expected halogen bonding interactions. In several cases halide ion acceptors were also engaged in complementary hydrogen bonding interactions with C–H groups of pyridinium rings and O–H groups of water solvates. Halogen bond donors containing a diiodophenyl group formed either an extended network or discrete supramolecular macrocyclic constructs through ArI···Cl$^-$···IAr bridging interactions. Significantly fewer and weaker halogen bonding interactions were observed in crystals of *N*-bromophenylpyridinium salts. The attenuation of halogen bonding in these substrates is attributed to the inability of the activated bromoarene halogen bond donors to compete with hydrogen bond donors (C–H/O–H residues) for the halide anion.

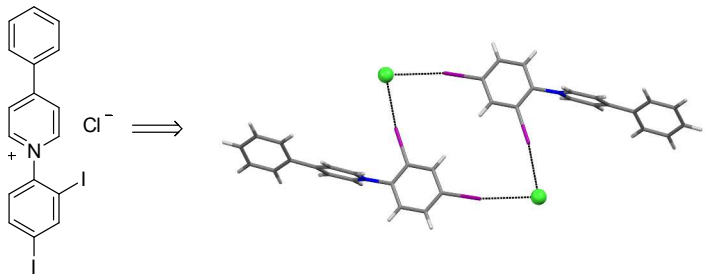

F. Christopher Pigge
Department of Chemistry
University of Iowa
Iowa City, Iowa 52242
Ph: 319-335-3805
Fax: 319-335-1270
Email: chris-pigge@uiowa.edu

Charge-Assisted Halogen Bonding in Bromo- and Iodophenylpyridinium Chlorides

*Christopher J. Kassl, Dale C. Swenson, and F. Christopher Pigge**

Department of Chemistry, University of Iowa, Iowa City, Iowa, 52242, USA

ABSTRACT: Ten *N*-halophenylpyridinium salts (halogen = Br or I) with chloride (and in one case iodide) counterions have been prepared and structurally characterized in order to examine the degree of solid state halogen bonding exhibited in these systems. *N*-Halophenylpyridinium salts are easily synthesized from existing pyridines, and the cationic pyridinium group is expected to increase the halogen bond donor ability of attached halophenyl moieties. Halide anions functioning as halogen bond acceptors facilitate formation of charge-assisted halogen bonds. All five substrates featuring iodophenyl or diiodophenyl substituents displayed the expected halogen bonding interactions. In several cases halide ion acceptors were also engaged in complementary hydrogen bonding interactions with C–H groups of pyridinium rings and O–H groups of water solvates. Halogen bond donors containing a diiodophenyl group formed either an extended network or discrete supramolecular macrocyclic constructs through ArI···Cl^-···IAr bridging interactions. Significantly fewer and weaker halogen bonding interactions were observed in crystals of *N*-bromophenylpyridinium salts. The attenuation of halogen bonding in these substrates is attributed to the inability of the activated bromoarene halogen bond donors to compete with hydrogen bond donors (C–H/O–H residues) for the halide anion.

INTRODUCTION

Halogen bonding interactions have emerged as important non-covalent attractions capable of facilitating molecular recognition and self-assembly events in both solution phase and the solid state.[1] For example, halogen bonding (XB) interactions have been utilized in the design of numerous functional materials,[2] as the principal recognition element of molecular hosts targeting halocarbon and anionic guests,[3] and as the operative feature in new organocatalysts.[4] Likewise, in the solid state designed XB interactions have been used to mediate self-assembly of numerous intriguing organic and inorganic crystalline materials.[5,6] While XB remains much less exploited in supramolecular chemistry compared to hydrogen bonding, halogen bonding clearly represents an increasingly important design tool for control over a variety of non-covalent assembly processes.

The basis for halogen bonding is generally regarded as an electrostatic attraction between an electrophilic halogen bond donor and a Lewis base (LB) halogen bond acceptor.[7] Many organohalogens feature an uneven distribution of electron density about the halogen such that a region of positive electrostatic potential exists directly opposite the C–X bond axis.[8] An attractive interaction between this region of positive electrostatic potential and an electron rich Lewis basic site constitutes a halogen bond. Much of what is known about the strength of halogen bonds has been inferred from crystallographic studies in which halogen bonding is indicated by X···LB distances shorter than the sum of the relevant van der Waals radii and C–X···LB angles approaching 180°.[1,7,8] Recently, several studies have examined the strength of halogen bonding in solution by NMR spectroscopy.[9]

Computational and experimental studies consistently show that organo-halogen bond donor ability follows the order RI > RBr > RCl as a consequence of increasing polarizability of the heavier halogens.[1,7,8] Importantly, carbon hybridization and electron-withdrawing inductive effects exerted by nearby substituents can further enhance XB donor ability of R–X groups. Indeed, while relatively simple "unactivated" organohalogens are not particularly good XB donors, iodo-alkynes, perfluoro-iodoalkanes, and perfluoro-iodoarenes are among the best halogen bond donors.[10] However, the ability to incorporate these activated halogen bonding motifs into larger molecules with the aim of influencing self-assembly via halogen bonding can be difficult. Thus, the identification of additional synthetically accessible halo-organic moieties that exhibit structure directing effects as a consequence of reliable halogen bond donor ability may further expand the role of halogen bonding in supramolecular chemistry and crystal engineering.

In formulating strategies to construct modular XB donors amenable to potential incorporation into larger supramolecular building blocks, we were attracted to the use of pyridinium cations as activating groups toward covalently attached haloaryl substituents. We reasoned that the pyridinium substituent would serve as a potent electron-withdrawing group to activate the attached halophenyl moieties. Moreover, N-halophenyl pyridinium cations should be easily accessed via manipulation of pre-existing pyridine rings. In turn, any molecule possessing a peripheral pyridine substituent might then be converted to a potential XB donor. Notably, the superior XB donor ability of cationic iodo- and bromo-azolium salts (e.g., halopyridinium and haloimidazolium salts) has been amply demonstrated in a number of studies.[3c-i,4,9a,11] The cationic halogen bond donors envisioned in this study, however, differ from halopyridinium donors in that the halogen is not directly attached to the pyridine ring, but instead is present on

an *N*-aryl moiety. Indirect support for the notion of *N*-halophenylpyridinium derivatives as XB donors can be found in studies examining solid state halogen bonding interactions in positively charged haloanilinium salts (i.e., $XC_6H_4NH_3^+$).[12] Notably, the presence of a competitive hydrogen bond donating group in the form of the NH_3^+ fragment is a complicating factor in these studies. The *N*-halophenylpyridinium derivatives investigated in this this study lack such potent H-bond donors. Further evidence for halogen bonding activating effects of pyridinium cations can be found in solid state structures of bis(halobenzyl)bipyridinium and bis(halophenyl)imidazolium salts.[13]

We describe below results of a preliminary investigation probing the halogen bonding behavior of nine iodophenyl- and bromophenylpyridinium chlorides (Chart 1). Both mono- and dihalophenylpyridinium chlorides have been structurally characterized to assay the propensity for formation of discrete charge-assisted X···Cl$^-$ halogen bonds as well as bridging X···Cl$^-$···X interactions leading to extended solid state networks with chloride anions functioning as XB acceptors in each case. One substrate (**5**) was obtained in crystalline form as the iodide salt, and structural details of this material are also presented.

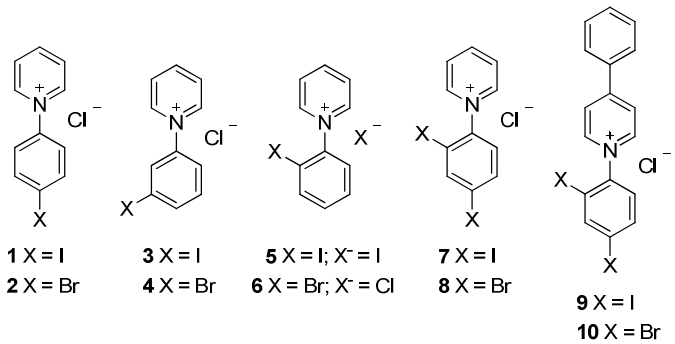

Chart 1. *N*-halophenylpyridinium chlorides structurally characterized in this study.

EXPERIMENTAL SECTION

General procedure for the preparation of *N*-halophenylpyridinium salts

The route is outlined in Scheme 1. Zincke salt **11**[14] (0.5 mmol) and the appropriate haloaniline (0.75 mmol) were combined along with 5.0 mL of n-butanol in a 10 mL round bottom flask. The mixture was heated to reflux with stirring under Ar and maintained for 3 d. After this time analysis of the reaction mixture by LRMS indicated complete disappearance of Zincke salt **11**. The solvent was evaporated under reduced pressure and the crude material was dissolved in a minimum amount of methanol and added dropwise to a solution of diethyl ether (200 mL). The resulting precipitate was collected by filtration and washed sequentially with diethyl ether and ethyl acetate until washings became clear in color, and then dried under vacuum.

The salts are all insoluble in most organic solvents, but exhibit good solubility in methanol and n-butanol. They are sparingly soluble in acetone and water.

X-ray Crystallography

Single crystals of N-halophenylpyridinium salts **1-10** were grown by dissolving 5 mg of the salt in ~1 mL of an acetone:methanol solution (1:1) inside a 20-mL borosilicate glass screw cap scintillation vial. After 1-2 days of slow solvent evaporation at room temperature, crystals suitable for single crystal X-ray diffractometry were obtained.

Diffraction data were collected on a Nonius Kappa CCD diffractometer equipped with Mo Kα radiation with λ = 0.71073 Å. Crystallographic data is shown in Tables 1 and 2. Select details on structure solution and refinement are described below and full details can be found in the Supporting Information (CIF).

10•$(H_2O)_{\sim 1.5}$. The structure contains two sites partially occupied by chloride counterion and water solvate. One site (O3-Cl7) was refined to 0.671(4) occupancy while the other site (O4-Cl6) refined to 0.571(8) occupancy. Atoms in each respective site were modeled with the same anisotropic displacement parameters. Hydrogen bond distances to O1 and O2A were restrained to 0.85 Å. The position of hydrogen atoms bonded to O4 was not successfully modeled but their presence is inferred.

***N*-4-Iodophenylpyridinium chloride (1)**

Yield: 77% as light brown powder; mp: >220^{0}C. ^{1}H NMR (d_4-MeOH, 300 MHz) δ: 9.24 (d, 2H, *J* = 6.9 Hz), 8.79 (t, 1H,), 8.30 (dt, 2H), 8.12 (d, 2H, *J* = 6.9 Hz), 7.60 (d, 2H, *J* = 6.9 Hz). ^{13}C NMR (d_4-MeOH, 75 MHz) δ: 148.2, 146.0 141.0, 129.6, 127.3, 98.8. HRMS (ESI): 281.9780 calculated for $C_{11}H_9NI$ $[M]^+$: found 281.9785.

***N*-4-Bromophenylpyridinium chloride (2)**

Yield: 73% as cream-colored powder; mp: >220^{0}C. ^{1}H NMR (d_4-MeOH, 300 MHz) δ: 9.32 (d, 2H, *J* = 6.9 Hz), 8.86 (t, 1H), 8.35 (dt, 2H), 7.98 (d, 2H, *J* = 6.9 Hz), 7.84 (d, 2H, *J* = 6.9 Hz). ^{13}C NMR (d_4-MeOH, 75 MHz) δ: 148.2, 146.1, 142.5, 134.8, 129.6, 127.5 127.0. HRMS (ESI): 233.9918 calculated for $C_{11}H_9NBr$ $[M]^+$; found 233.9923.

***N*-3-Iodophenylpyridinium chloride (3)**

Yield: 85% as light brown powder; mp: >220^{0}C. ^{1}H NMR (d_4-MeOH, 300 MHz) δ: 9.24 (d, 2H, *J* = 6.0 Hz), 8.80 (t, 1H), 8.31-8.26 (m, 3H), 8.12 (d, 1H, *J* = 8.1 Hz), 7.85 (d, 1H, *J* = 8.1 Hz), 7.50 (t, 1H). ^{13}C NMR (d_4-MeOH, 75 MHz) δ: 148.3, 146.1, 142.0, 134.5, 133.0, 129.6, 125.2, 95.4. HRMS (ESI): 281.9780 calculated for $C_{11}H_9NI$ $[M]^+$; found 281.9788.

***N*-3-Bromophenylpyridinium chloride (4)**

Yield: 63% as light yellow powder; mp: >220^{0}C. ^{1}H NMR (d_4-MeOH, 300 MHz) δ: 9.26 (d, 2H, *J* = 6.9 Hz), 8.86 (t, 1H), 8.35 (t, 2H), 8.14 (d, 1H, *J* = 2.1 Hz), 7.96 (d, 1H, *J* = 8.1 Hz), 7.87 (dd, 1H), 7.68 (t, 1H). ^{13}C NMR (d_4-MeOH, 75 MHz) δ: 149.7, 147.5, 142.5, 137.1, 134.5, 130.9, 130.2, 126.1, 125.8. HRMS (ESI): 233.9918 calculated for $C_{11}H_9NBr$ $[M]^+$; found 233.9922.

***N*-2-Iodophenylpyridinium iodide (5)**

Yield: 38% as dark brown powder; mp: >220^{0}C. ^{1}H NMR (d_4-MeOH, 300 MHz) δ: 9.20 (d, 2H, *J* = 6.0 Hz), 8.91 (t, 1H), 8.41 (t, 2H), 8.26 (d, 1H, *J* = 8.1 Hz), 7.82 (m, 2H), 7.53 (t, 1H). ^{13}C NMR (d_4-MeOH, 75 MHz) δ: 148.0, 146.3, 138.9, 135.5, 134.5, 131.0, 129.7, 128.6, 98.3. HRMS (ESI): 281.9780 calculated for $C_{11}H_9NI$ $[M]^+$; found 281.9783.

N-2-Bromophenylpyridinium chloride (6)

Yield: 68% as bright yellow powder; mp: >220^{0}C. ^{1}H NMR (d_4-MeOH, 300 MHz) δ: 9.18 (d, 2H, *J* = 6.9 Hz), 8.86 (t, 1H), 8.35 (t, 2H), 7.97 (t, 1H), 7.86 (d, 1H, *J* = 8.1 Hz), 7.96 (d, 1H, *J* = 8.1Hz), 7.76-7.64 (m, 2H). ^{13}C NMR (d_4-MeOH, 75 MHz) δ: 149.3, 147.7, 137.4, 135.5, 134.6, 130.8, 129.7, 128.9, 115.7. HRMS (ESI): 233.9918 calculated for $C_{11}H_9NBr$ $[M]^+$; found 233.9926.

***N*-2,4-Diiodophenylpyridinium chloride (7)**

Yield: 32% as dark brown powder; mp: >220^{0}C. ^{1}H NMR (d_4-MeOH, 300 MHz) δ: 9.15 (d, 2H, *J* = 6.1 Hz), 8.91 (t, 1H), 8.58 (d, 1H, *J* = 2.4 Hz), 8.38 (t, 2H), 8.11 (dd, 1H), 7.56 (d, 1H, *J* = 8.1Hz). ^{13}C NMR (d_4-MeOH, 75 MHz) δ: 148.1, 146.1, 139.3, 128.4, 127.8, 98.1, 94.8. HRMS (ESI): 407.8746 calculated for $C_{11}H_8NI_2$ $[M]^+$; found 407.8754.

***N*-2,4-Dibromophenylpyridinium chloride (8)**

Yield: 71% as light yellow powder; mp: >220^{0}C. ^{1}H NMR (d_4-MeOH, 300 MHz) δ: 9.17 (d, 2H, *J* = 6.0 Hz), 8.89 (t, 1H), 8.36 (t, 2H), 8.13 (d, 1H, *J* = 2.1 Hz), 7.92 (dd, 1H), 7.77 (d, 1H, *J* = 8.1 Hz). ^{13}C NMR (d_4-MeOH, 75 MHz) δ: 149.6, 147.7, 137.8, 134.0, 130.1, 129.7, 127.6, 115.7. HRMS (ESI): 311.9024 calculated for $C_{11}H_8NBr_2$ $[M]^+$; found 311.9034.

4-Phenyl-*N*-2,4-diiodophenylpyridinium chloride (9)

Yield: 34% as dark brown powder; mp: >220^{0}C. ^{1}H NMR (d_4-MeOH, 300 MHz) δ: 9.13 (d, 2H, *J* = 6.1 Hz), 8.71 (d, 2H, *J* = 6.1 Hz), 8.65 (d, 1H, *J* = 2.1 Hz), 8.20 (m, 3H), 7.77 (m, 3H), 7.60 (d, 1H, *J* = 8.1 Hz). ^{13}C NMR (d_4-MeOH, 75 MHz) δ: 149.6, 147.3, 144.4, 140.6, 139.5, 134.8, 134.3, 131.2, 129.6, 129.3, 126.1, 98.2, 94.8. HRMS (ESI): 483.9059 calculated for $C_{17}H_{12}NI_2$ $[M]^+$; found 483.9071.

4-Phenyl-*N*-2,4-dibromophenylpyridinium chloride (10)

Yield: 44% as light yellow powder; mp: >220^{0}C. ^{1}H NMR (d_4-MeOH, 300 MHz) δ: 9.10 (d, 2H, *J* = 6.9 Hz), 8.65 (d, 2H, *J* = 6.9 Hz), 8.26 (d, 1H, *J* = 2.1 Hz), 8.12 (d, 2H, *J* = 8.7 Hz), 7.95 (dd, 1H), 7.77 (d, 1H, *J* = 8.1 Hz), 7.69-7.71 (m, 3H). ^{13}C NMR (d_4-MeOH, 75 MHz) δ: 147.3, 142.5, 137.8, 134.8, 134.2, 134.1, 133.0, 131.2, 130.3, 129.7, 127.5, 126.1, 120.7. HRMS (ESI): 387.9332 calculated for $C_{17}H_{12}NBr_2$ $[M]^+$; found 387.9339.

Table 1. Crystallographic data for *N*-halophenylpyridinium salts **1**-**5**.

	***1*•$(H_2O)_2$**	***2*•$(H_2O)_{1.5}$**	***3*•$(H_2O)_{0.5}$**	***4*•$(H_2O)_{0.5}$**	***5***
Crystallization Yield (%)	88	85	89	83	77
Formula	$C_{11}H_{13}ClINO_2$	$C_{11}H_{12}BrClNO_{1.5}$	$C_{11}H_{10}ClINO_{0.5}$	$C_{11}H_{10}BrClNO_{0.5}$	$C_{11}H_9I_2N$
Formula weight	353.57	297.58	326.56	279.35	408.99

Crystal system	monoclinic	monoclinic	tetragonal	triclinic	monoclinic
Space group	$P2_1/c$	$P2_1/n$	$P4_12_12$	P-1	$P2_1/c$
a/Å	8.9791(5)	17.0693(12)	8.3557(6)	7.4154(4)	13.6280(14)
b/Å	7.4795(4)	7.4556(5)	8.3557(6)	11.0476(6)	6.9633(7)
c/Å	19.7533(11)	19.5710(13)	34.1012(3)	13.9173(8)	13.4276(13)
$\alpha/^0$	90	90	90	102.3083(14)	90
$\beta/^0$	96.2197(12)	102.9486(17)	90	95.2744(13)	102.5700(12)
$\gamma/^0$	90	90	90	90.0762(12)	90
V/Å^3	1318.8(2)	2427.3(5)	2380.9	1108.97	1243.69(15)
Z	4	8	8	4	4
D_{calc}	1.781	1.629	1.822	1.674	2.184
μ (mm^{-1})	2.617	3.586	2.887	3.918	5.021
T/K	190(2)	190(2)	190(2)	190(2)	190(2)
No. of reflections	17377	38104	41165	13789	16298
No. of unique reflections	2507	5214	3373	5120	2294
No. of reflections with $I > 2\sigma(I)$	2357	4029	3207	4425	2014
No. of params.	161	304	136	265	127
R_1 [$I > 2\sigma(I)$]	0.0257	0.0293	0.0178	0.0254	0.0372
wR_2	0.0955	0.1028	0.0464	0.0923	0.1273
CCDC No.	1052260	1052261	1052262	1052263	1052264

Table 2. Crystallographic data for *N*-halophenylpyridinium salts **6-10**.

	6•(H$_2$O)	***7•(H$_2$O)$_{1.5}$***	***8•(H$_2$O)$_2$***	***9***	***10•(H$_2$O)$_{\sim 1.5}$***
Crystallization yield (%)	80	73	90	75	86
Formula	$C_{11}H_{11}BrClNO$	$C_{11}H_{11}ClI_2NO_{1.5}$	$C_{11}H_{12}Br_2ClNO_2$	$C_{17}H_{12}ClI_2N$	$C_{17}H_{13.39}Br_2Cl_{1.11}NO_{0.89}$
Formula weight	288.56	470.46	385.49	519.53	445.15
Crystal system	monoclinic	monoclinic	monoclinic	monoclinic	triclinic
Space group	$P2_1/n$	C2/c	$P2_1/c$	C2/c	P-1
a/Å	8.4925(11)	31.759(2)	10.4651(5)	9.2519(4)	9.9620(6)
b/Å	9.9455(13)	9.0729(7)	8.5805(3)	19.9679(10)	11.8679(13)
c/Å	13.5872(19)	19.9453(14)	16.0117(7)	19.1621(9)	16.181(2)
α/^{0}	90	90	90	90	107.803(6)
β/^{0}	90.684(3)	90.4430(13)	107.987(2)	99.712(2)	98.300(6)
γ/^{0}	90	90	90	90	105.069(6)
V/Å^3	1147.5(5)	5747.1(12)	1367.52(15)	3489.3(4)	1705.9(4)
Z	4	16	4	8	4
D_{calc}	1.670	2.175	1.872	2.008	1.719
μ (mm^{-1})	3.786	4.544	6.112	3.755	4.908
T/K	190(2)	190(2)	190(2)	190(2)	190(2)

No. of reflections	15431	35759	22401	19769	19097
No. of unique reflections	2105	6940	3280	3343	6202
No. of reflections with $I > 2\sigma(I)$	1422	5855	2767	2923	2698
No. of params	144	307	155	192	417
R_1 [$I > 2\sigma(I)$]	0.0434	0.0255	0.0311	0.0366	0.0653
wR_2	0.1210	0.0811	0.1028	0.1241	0.1674
CCDC No.	1052265	1052266	1052267	1052268	1052269

RESULTS AND DISCUSSION

The synthesis of halophenylpyridinium halides **1**-**10** was accomplished using the general route illustrated in Scheme 1. Pyridine and 4-phenylpyridine were converted to the corresponding Zincke salts **11** in good yield by treatment with 1-chloro-2,4-dinitrobenzene according to published procedures.[14] Simply heating **11** with the appropriate halo- or dihaloaniline in n-BuOH afforded the desired halophenylpyridinium chlorides **1**-**4** and **6**-**10** in moderate to good isolated yields.[15] Initial attempts to prepare these materials in a lower boiling solvent (EtOH) were unsuccessful, and in one case an intermediate arising from pyridine ring opening was obtained.[16] In the reaction of **11** with 2-iodoaniline, the desired *N*-(2-iodophenyl)pyridinium cation was obtained as the iodide salt. Evidently, the iodoaniline and/or a portion of the 2-iodophenylpyridinium cation suffered de-halogenation under the reaction

conditions to provide the iodide anions observed in the crystalline salts. None of the other substrates exhibited any evidence of similar de-halogenation processes. Each salt was spectroscopically characterized by $^{1}H/^{13}C$-NMR and positive ion ESI-HRMS. In each case X-ray quality single crystals were grown by slow evaporation of mixed MeOH/acetone solutions. Crystalline samples were characterized by single-crystal X-ray diffractometry and PXRD.

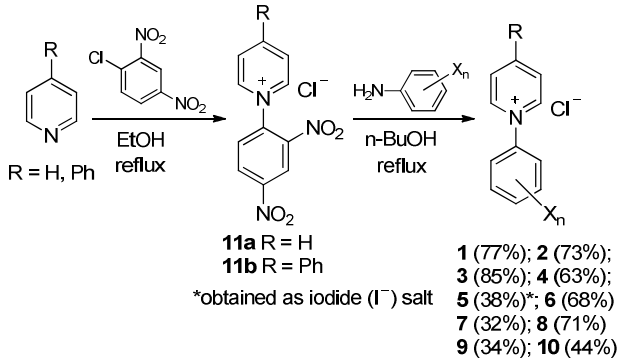

Scheme 1. Route used to prepare *N*-halophenylpyridinium salts **1-10**.

At the outset, we expected the electron-withdrawing pyridinium substituents to activate halophenyl groups toward halogen bonding to varying degrees according to the identity of the halogen (Br versus I) and substitution pattern (*o*, *m*, *p*). The ability of halide anions (e.g., Cl^{-}) to serve as halogen bond acceptors is well-documented, so it was further expected that any halogen bonding observed would be of the charge-assisted variety.[1e,3c,17] While substrates **1-10** are devoid of conventional hydrogen bond donors, we recognized that solid state aryl and pyridinium C–H···X^{-} hydrogen bonding may be competitive with halogen bonding. Additionally, solubility features of **1-10** required use of polar solvent mixtures in crystallization experiments and so the potential presence of hydrogen bonding solvates (methanol, adventitious H_2O) was also a complicating feature.

The structure of 4-iodophenylpyridinium chloride (**1**) embodies many of the considerations outlined above. The ion pair **1** and two water molecules of solvation comprise the asymmetric

unit (Figure 1). A halogen bonding interaction is clearly evident as indicated by the ratio of the observed I···Cl^- distance (3.436 Å) over the sum of the relevant van der Waals radii (3.79 Å): R_{XB} = 0.91.[18] Additionally, the C–I···Cl^- angle is close to linear (166.27º) and the metrics of this XB interaction are similar to those observed in the structure of 4-iodoanilinium chloride reported previously.[12b] The two water molecules are engaged with the Cl^- ion via hydrogen bonding and are part of an extensive network of solvated chloride ions as shown in Figure 2. Hydrogen bonding between chloride ions and water solvates produces fused cyclic motifs linked by iodophenylpyridinium cations via I···Cl^- halogen bonding and pyridinium C–H···OH_2 hydrogen bonding to give 2D layers. Iodophenylpyridinium cations are stacked in a head-to-tail manner consistent with favorable dipolar alignment. Centroid–centroid distances between stacked iodophenyl and pyridinium rings are within range of π–π interactions (3.783 Å). The layers evident in Figure 2 stack in slightly offset fashion and are linked by additional C–H···Cl^- hydrogen bonding (see Figure S1 in the Supporting Information). Thus, the overall packing features segregated stacks of 4-iodophenylpyridinium cations separated by channel-type networks of solvated chloride ions (Figure S2).[19]

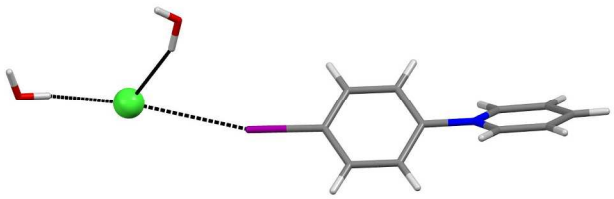

Figure 1. Asymmetric unit in **1**. Chloride anion shown as green sphere. I···Cl^- *d* = 3.436 Å, R_{XB} = 0.91, C–I···Cl^- = 166.27º.

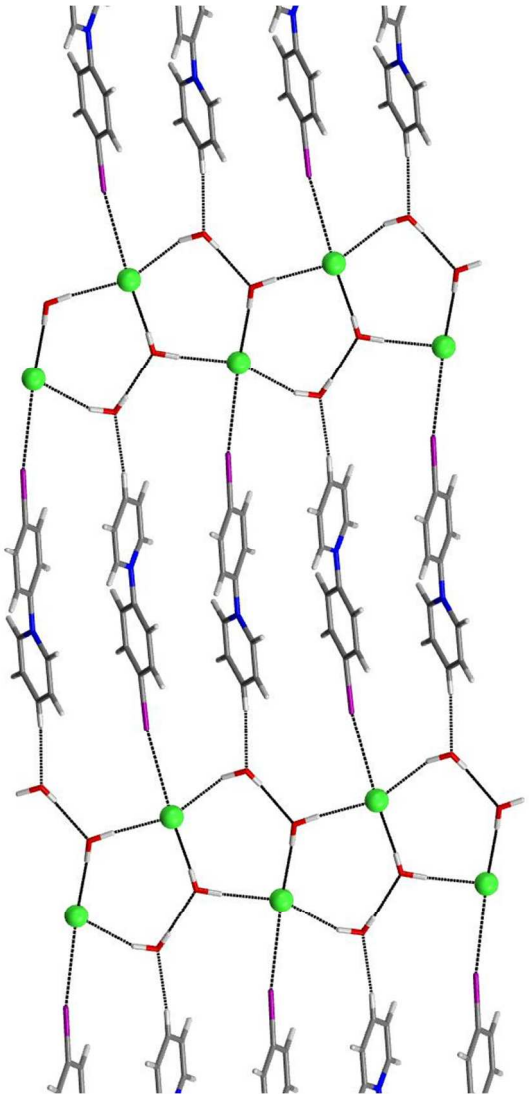

Figure 2. Interplay of XB and chloride ion solvation in **1**.

The structure of 4-bromophenylpyridinium chloride (**2**) differs from the iodo analogue in several ways. Firstly, two unique pyridinium cations are present in the asymmetric unit. Only one of these is engaged in Br···Cl^- halogen bonding, and the Br···Cl^- distance (3.490 Å, R_{XB} = 0.95) is indicative of a relatively weak interaction (Figure 3). The aryl bromide of the second cation participates in a bifurcated interaction in which the bromine functions as a halogen bond donor to a water solvate molecule (Br···O 3.271 Å, R_{XB} = 0.97, C–Br···O angle 163.53º) and a

hydrogen bond acceptor to a pyridinium C-H donor (H···Br distance 3.016 Å, C–Br···H angle 142.36º). Similar to the structure of **1**, the chloride ions are present as part of cylic hydrated networks linked by bridging bromophenyl pyridinium cations (through $Br\cdots Cl^{-}/OH_2$ halogen bonding and pyridinium $C–H\cdots Cl^{-}/OH_2$ hydrogen bonding) to form 2D layers. In turn, these layers are arranged in an offset fashion to afford stacks of pyridinium cations separated by hydrated choride ion networks (Figure S5, very similar to the overall packing observed in **1**). Within individual stacks the aryl pyridinium cations adopt a favorable dipolar alignment with arene – arene separations ranging from 3.786 Å to 3.914 Å.

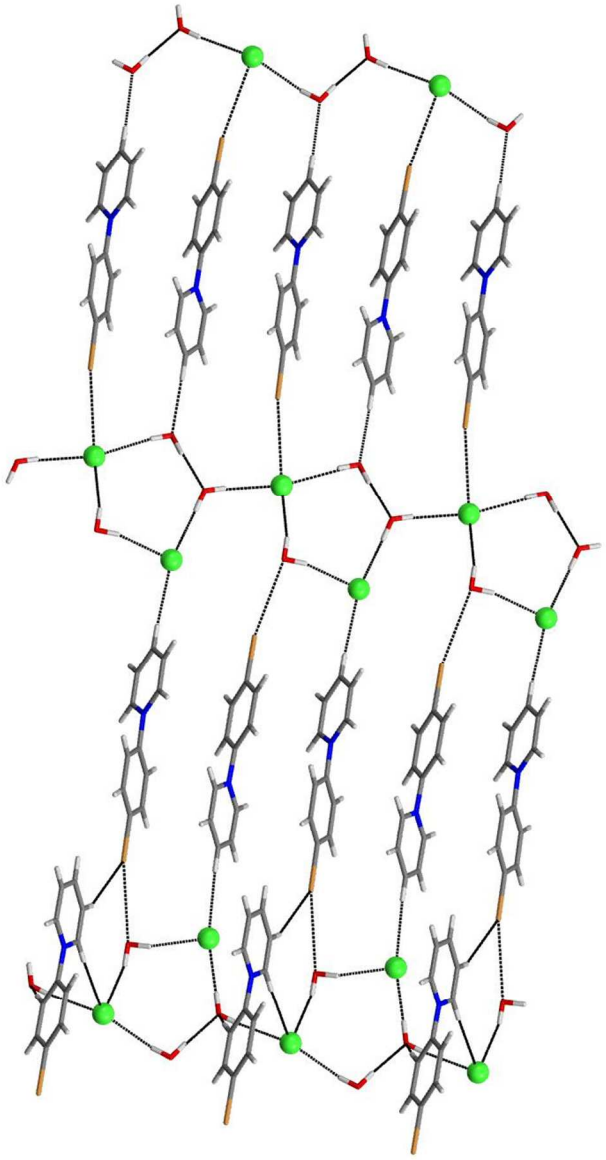

Figure 3. Halogen and hydrogen bonding interactions in **2**. See text for XB and HB metrics.

The structure of 3-iodophenylpyridinium chloride (**3**) features one ion pair and 0.5 H_2O solvate in the asymmetric unit. Each chloride anion exhibits six intermolecular contacts, one of which is a relatively strong halogen bond to an iodoarene moiety (I···Cl^- distance 3.249 Å, R_{XB} = 0.86, C–I···Cl^- angle 168.01º). Aryl and pyridinium C–H···Cl^- hydrogen bonds from four additional pyridinium cations and a hydrogen bond from a chloride-bridging water molecule

complete the coordination sphere of the anion (Figure 4). The overall packing in the crystal is quite complicated, and the arylpyridinium cations are not engaged in intermolecular stacking interactions as was observed in **1** and **2** (see Figure S6). Nonetheless, a notable feature of this structure is the presence of relatively strong halogen bonding interactions that involve each iodoarene group. Notably, these I···Cl^- interactions are shorter than those observed in the structure of **1** (*vide supra*) and in a related 4-iodoanilinium chloride salt.[12b]

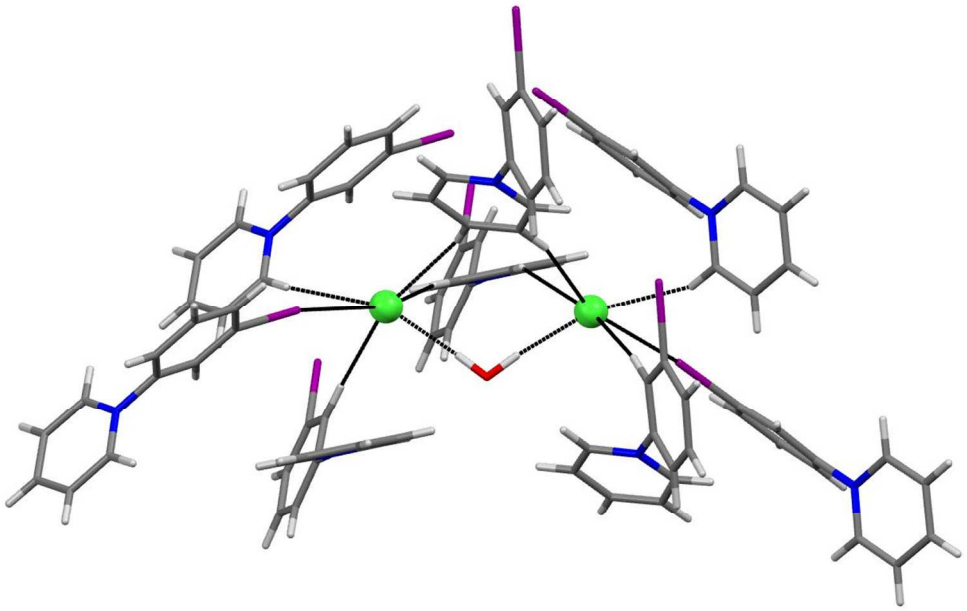

Figure 4. Intermolecular interactions of chloride ions in **3**.

In contrast, the structure of the 3-bromophenylpyridinium analogue (**4**) exhibits significantly fewer halogen bonding interactions. Indeed, as found in the structure of **2**, two unique ion pairs are present in the asymmetric unit (along with a water of solvation), and only one of these bromophenyl moieties is involved in halogen bonding to a chloride anion (labeled Br2A in Figure 5). Furthermore, the metrics of this interaction (Br···Cl^- distance 3.543 Å, R_{XB} = 0.97, C–Br···Cl^- angle 161.13°) indicate a relatively weak halogen bond. The second bromophenyl unit

(Br1) does not appear to participate in any significant intermolecular contacts. As was the case in the structure of **3**, chloride ions in **4** are organized in pairs through hydrogen bonding to a bridging water molecule, and each anion exhibits a roughly octahedral coordination sphere defined by O–H and C–H hydrogen bond donors, along with the single Br···Cl⁻ halogen bond. A further feature of this structure is the self-assembly of unique pyridinium cations into distinct linear chains via dipolar stacking of pyridinium and bromophenyl rings (Figure S7).

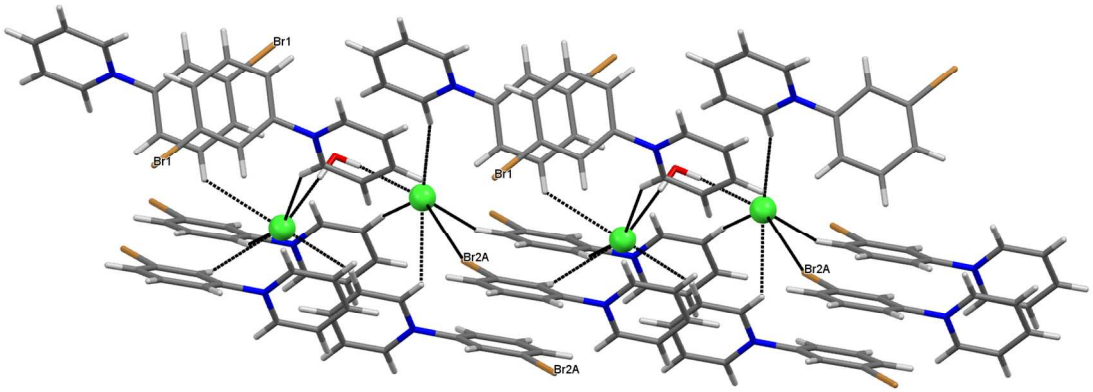

Figure 5. Coordination environment of chloride ions in **4**.

The 2-iodophenylpyridinium cation was found to crystallize with an iodide counterion (*vide supra*). Crystals of **5** were additionally obtained free of water solvate molecules, perhaps as a consequence of the increased hydrophobicity of iodide compared to chloride.[20] The asymmetric unit consists of one ion pair, and each iodoarene group is engaged in halogen bonding to an iodide anion (Figure 6, C–I···I⁻ 3.576 Å, R_{XB} = 0.86, 170.47°). This interaction is considerably shorter halogen bonds observed in crystals of 3-iodoanilinium iodide reported by Gray and Jones (3.691 Å).[12a] Each iodide anion exhibits six close intermolecular contacts. In addition to the halogen bond, four C–H···I⁻ hydrogen bonds are observed involving four different pyridinium cations. C–H groups on pyridinium rings serve as H-bond donors for three of these interactions,

and the fourth emanates from an iodophenyl C–H donor. Distances of these interactions range from 2.855 Å to 3.141 Å (I^-···H vdW distance = 3.26 Å). Each anion also approaches the face of a nearby cationic pyridinium ring (d = 3.669 Å) to complete the iodide coordination sphere. A view of the extended packing reveals that the iodide anions are well separated (closest I^-···I^- approach is > 6 Å) and reside in channels extending down the c axis (Figure S8).[21]

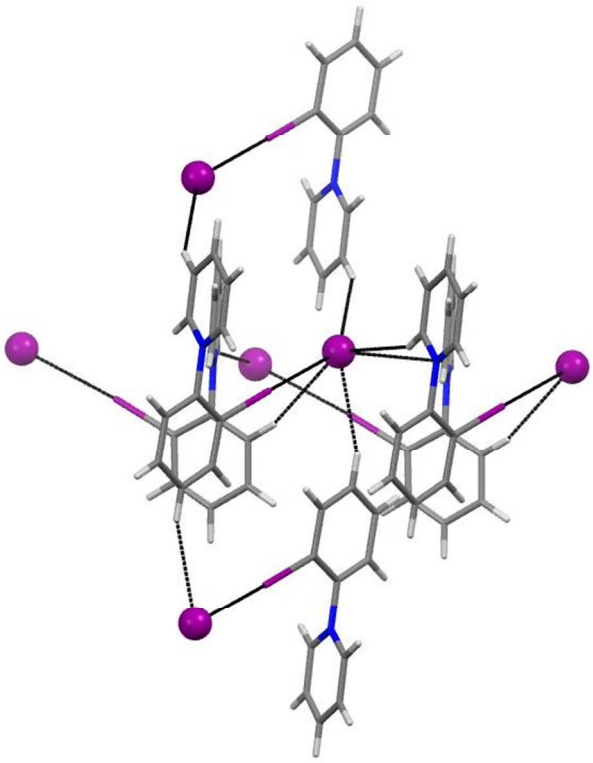

Figure 6. ArI···I^- halogen bonding and the coordination sphere around iodide in **5** (iodide anions shown as purple spheres).

The structure of 2-bromophenylpyridinium chloride (**6**) features little to no halogen bonding. Instead, chloride anions are organized in zig-zag chains mediated by hydrogen bonding to bridging water solvate molecules. Additional interactions involving pyridinium C–H···Cl^- hydrogen bonding are also evident as illustrated in Figure 7. The distance of the Br···Cl^- contact

shown in Figure 7 (light blue) is virtually equal to the sum of the van der Waals radii (d = 3.626 Å, Σ_{vdW} radii = 3.66 Å, R_{XB} = 0.99) and the C–Br···Cl^- angle is 158.02°. According to these metrics, this interaction can, at best, be described as only a very weak halogen bond.

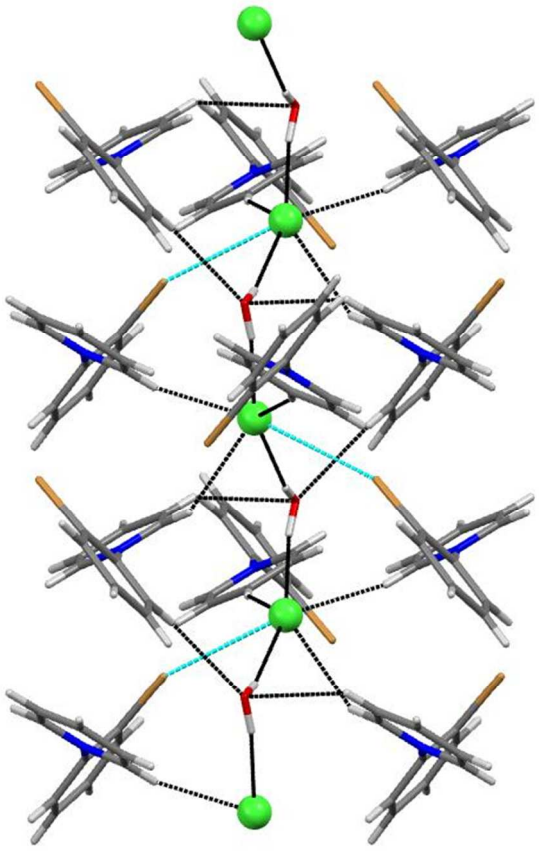

Figure 7. Non-covalent interactions surrounding the chloride ion in **6**. "Halogen bond" indicated in light blue is equal to the sum of the Br···Cl^- vdW radii.

The dihalophenylpyridinium chlorides **7-10** were chosen for study to explore generation of halogen bond-mediated networks. The introduction of a second halogen substituent in these substrates produces an excess of halogen bond donors relative to chloride halogen bond acceptors. Hence, the chloride ions may engage in halogen bonding with multiple halogen bond donors to produce extended networks and/or 0D oligomers (e.g., dimers, trimers, etc).[3c] Indeed,

the diiodophenylpyridinium derivatives **7** and **9** do, in fact, exhibit this solid state behavior, and these structures are discussed together below, followed by structural descriptions of dibromophenyl analogues **8** and **10**.

The asymmetric unit of diiodophenylpyridinium salt **7** contains two unique ion pairs and three water molecules of solvation. In the extended packing the unique arylpyridinium chlorides are segregated into individual, albeit similar, helical constructs mediated by bridging ArI···Cl^-···IAr halogen bonds. The metrics of halogen bonding interactions vary slightly between the two helices (see Figure 8) and the aryl–pyridinium torsion angles differ by ~10°. Each halogen bond indicated in Figure 8 approaches linearity with C–I···Cl^- angles ranging from 172.02° to 177.22°. The chloride ions bridge a 4-iodo substituent from one pyridinium cation and a 2-iodo substituent from a second pyridinium cation. The I···Cl^-···I angles are similar in both helical subunits (I1···Cl^-···I4 = 72.79° and I2···Cl^-···I3 = 75.95°). The two unique helical assemblies are linked by a network of bridging water molecules that connect chloride ions from one helix with chloride ions from the second helix (Figure 9). Aromatic C–H···Cl^- hydrogen bonding involving the most polarized pyridinium hydrogen atoms (adjacent to the nitrogen) also aid in mediating entanglement of the two helical networks.

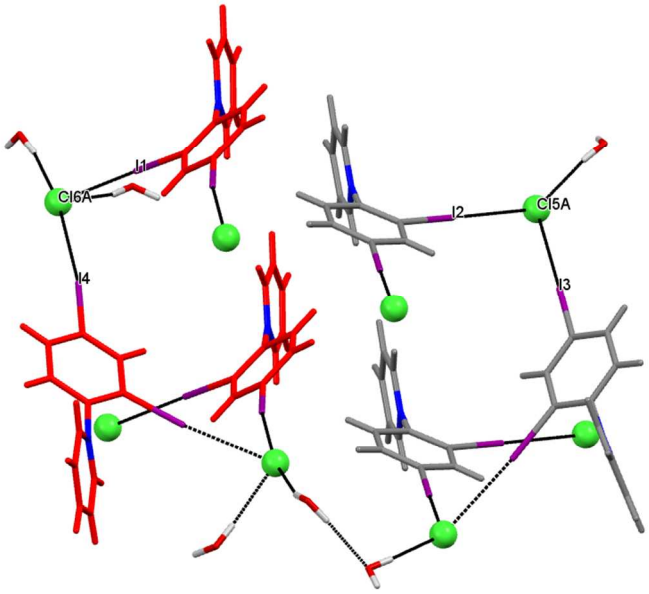

Figure 8. Extended halogen bonding networks in helical assemblies found in **7**. Helices derived from unique diiodophenylpyridinium cations are color coded red and grey. Halogen bonding metrics: I1···Cl6A$^-$ = 3.140 Å (R_{XB} = 0.83), I4···Cl6A$^-$ = 3.563 Å (R_{XB} = 0.94), C–I1–Cl6A$^-$ = 173.69º, C–I4–Cl6A$^-$ = 172.06º, I2···Cl5A$^-$ = 3.230 Å (R_{XB} = 0.85), I3···Cl5A$^-$ = 3.318 Å (R_{XB} = 0.88), C–I2–Cl5A$^-$ = 176.37º, C–I3–Cl5A$^-$ = 177.22º.

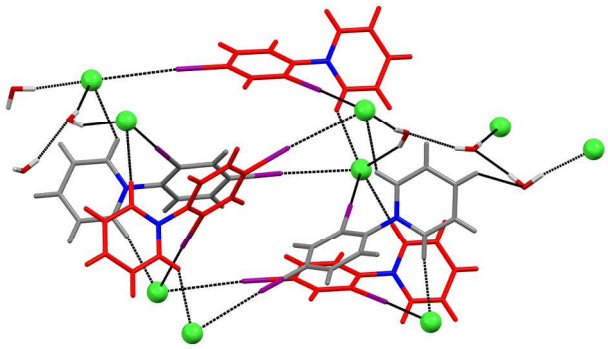

Figure 9. Bridging of unique helices in **7** through chloride ions by water solvates and C–H···Cl$^-$ hydrogen bonding.

The diiodophenyl-4-phenylpyridinium salt **9** also exhibits a halogen bonding network composed of ArI···Cl⁻···IAr bridging interactions. In this structure, however, no solvate molecules are found, perhaps a consequence of increased hydrophobicity upon introduction of the 4-phenyl substituent. Additionally, the halogen bonding network in this structure does not produce infinite chains of ion pairs, but instead results in formation of discrete halogen-bonded dimers that are arrayed in 2D layers (Figure 10).[22] The supramolecular macrocycles formed as a consequence of XB-mediated dimerization feature two distinct and relatively strong halogen bonds (I1···Cl = 3.232 Å, R_{XB} = 0.85, 169.39° and I2···Cl = 3.101 Å, R_{XB} = 0.82, 172.63°), and the I···Cl⁻···I angle is 81.44°. These halogen bonding metrics are comparable to those observed in XB-mediated macrocycles assembled from ammonium or phosphonium chlorides and the activated halogen bond donor 1,3,5-trifluoro-2,4,6-triiodobenzene.[22c] The Cl⁻···Cl⁻ separation across the halogen bonded dimers is 10.788 Å. Halogen bonded dimers are arrayed in the *bc* plane and are connected via pyridinium C–H···Cl⁻ hydrogen bonding (d = 2.575 Å) and dipole-assisted stacking interactions between the 4-phenyl substituents ($\pi_{cent}\cdots\pi_{cent}$ d = 3.879 Å). Halogen bonded layers in the *bc* plane are stacked in an ABAB pattern and are linked through additional C–H···Cl⁻ and C–H···I hydrogen bonding as shown in Figure 11. It should be noted that **7** and **9** possess an identical array of XB donor groups (2,4-diiodophenylpyridinium) and identical XB acceptors (Cl⁻), yet they exhibit much different halogen bonding networks. Thus, the presence of water solvate molecules in **7** and their absence in **9** appears to critically influence the observed halogen bonding motifs. Future research will examine the transferability of the chloride-bridged dimer synthon observed in **9** to other structurally related hydrophobic diiodophenylpyridinium derivatives.

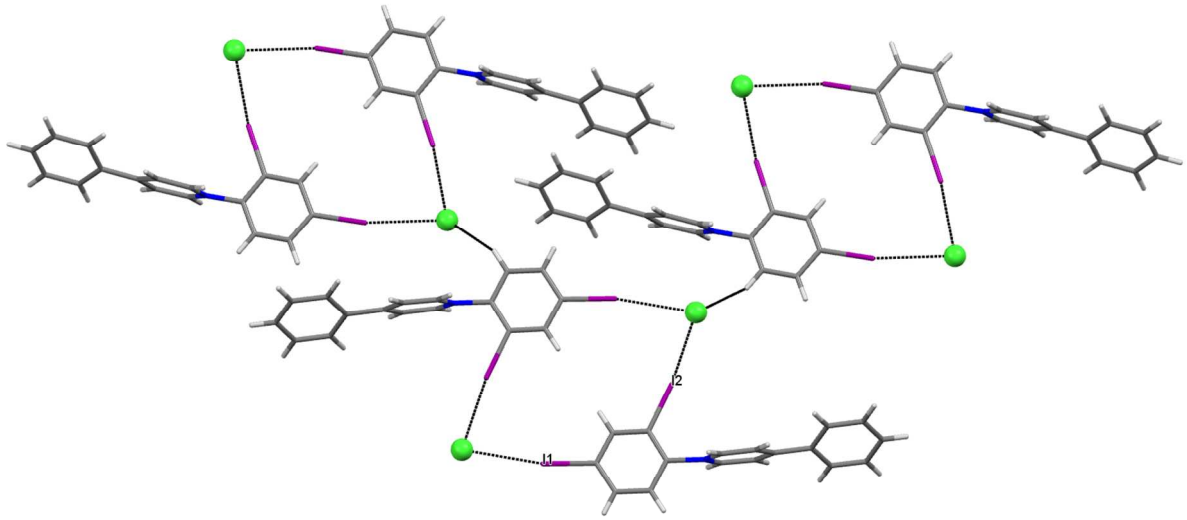

Figure 10. Halogen bonded macrocyclic dimers observed in **9**. See text for XB metrics.

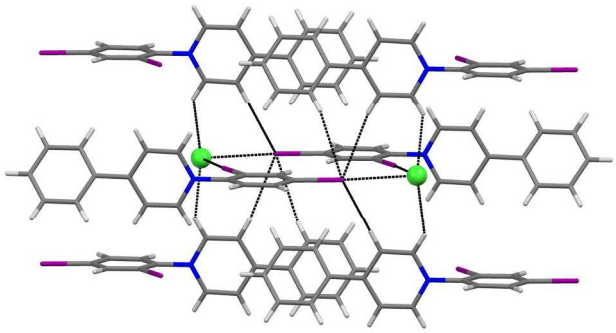

Figure 11. Stacking of layers shown in Figure 10 in an ABA fashion.

The structure of *N*-dibromophenylpyridinium salt **8** differs markedly from its diiodo analogue **7** in both crystalline network topology and degree of halogen bonding. Indeed, only the 2-bromo substituent of each phenylpyridinium cation exhibits any sort of halogen bonding interaction (involving a neighboring arene ring rather than the chloride anion, Figure 12), while the 4-bromo substituent does not engage in any significant intermolecular contacts. Each chloride accepts

two C–H hydrogen bonds from surrounding pyridinium rings. The remainder of the chloride coordination sphere is occupied by hydrogen bonding to water solvate molecules, in turn leading to an extensive network of water-bridged chlorides. Solvated chloride ions are segregated in alternating layers with the phenylpyridinium cations to produce an extended structure with well-defined hydrophilic and hydrophobic regions (Figure S11).

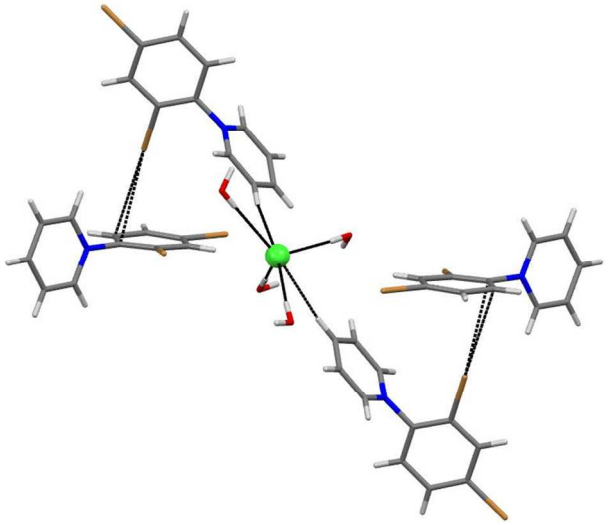

Figure 12. Environment around chloride ions in **8** and the absence of Br···Cl^- halogen bonds.

In contrast, certain solid state features found in the crystal structure of **10** bear similarity to features found in the diiodo analogue **9** discussed above, but important differences are also apparent. Most notably, each chloride ion in **10** is associated with a water of solvation, whereas the structure of **9** is solvate-free. The presence of solvated chloride ions gives rise to water-bridged chloride dimers mediated by O–H···Cl^- hydrogen bonding. Halogen bonding from bromoarene groups to both H_2O and Cl^- components of these dimers generate supramolecular macrocyclic assemblies of dibromophenylpyridinium cations that superficially resemble the chloride-bridged macrocycles observed in the structure of **9** (except for the participation of water solvate molecules). In these assemblies, the 2-bromo substituent engages a chloride ion in

halogen bonding (d = 3.286 Å, R_{XB} = 0.90, C–Br···Cl^- = 175.92°) while the 4-bromo substituent interacts with a Lewis basic oxygen of H_2O (Br···O d = 3.040 Å, R_{XB} = 0.90, C–Br···O = 167.94º) (Figure 13). Chloride ions exhibit additional C–H···Cl^- contacts to phenylpyridinium cations to extend the structure into three dimensions. The asymmetric unit of **10** contains a second ion pair along with an associated water of solvation. Chloride ions are arrayed in a zig-zag chain mediated by hydrogen bonding water molecules. Positional disorder between the chloride ions and water molecules, however, is a complicating feature. Dibromophenylpyridinium cations are positioned about the H_2O/Cl^- chain and engage in both halogen bonding and C–H···Cl^-/O hydrogen bonding (Figure S12). These two distinct networks are then arranged in undulating parallel layers in the extended packing (see Figure S13).

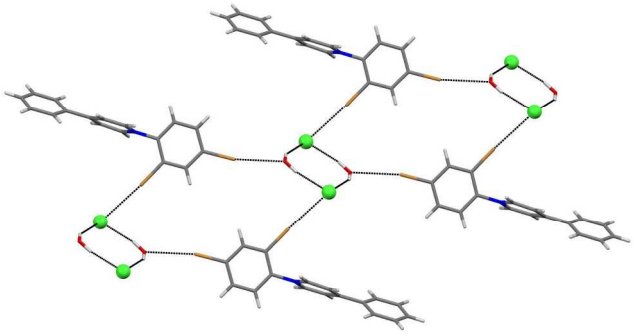

Figure 13. Principal hydrogen/halogen bonding network in **10**.

This study was initiated with the aim of assessing the feasibility of halophenylpyridinium groups to engage in significant halogen bonding with halide anion XB acceptors, and to further probe the utility of these interactions in mediating formation of discrete halogen bonding networks when the XB donor:acceptor ratio = 2. In this context comparison of the iodophenylpyridinium salts with their bomophenyl analogues reveals significant differences in the type, extent, and magnitude of solid state XB interactions. Specifically, every iodoarene

group in the substrates examined participates in solid state halogen bonding with chloride (or iodide in **5**) anions. This was largely anticipated as the activated iodoarenes are the sole halogen bond donors in these substrates and the halide anions are the best halogen bond acceptors.[23] The observed ArI···X^- interactions all exhibit R_{XB} of ~ 0.90 or less and C–I···X^- angles close to 180º. In contrast, several structures incorporating bromophenylpyridinium cations feature ArBr residues that do not engage in any significant intermolecular contacts. Moreover, in cases where ArBr···Cl^- contacts are evident, the Br···Cl^- R_{XB} are frequently only 0.99 – 0.95 (the structure of **10** providing an exception to this trend). Thus, while *N*-iodophenylpyridinium cations appear to be reliable halogen bond donors toward chloride and iodide anion acceptors, the analogous interaction between *N*-bromophenylpyridinium cations and chloride anions appears to be much less significant.

Differences in the interplay between halogen bonding and solvation as a function of halogen bond donor are also evident. Chloride anions possess relatively high energies of solvation, so it is not surprising that many of the salts examined in this study crystallize as hydrates (especially given the hydrophilic solvents used to grow crystals). Nonetheless, the presence of chloride-coordinated hydrate molecules proved compatible with halogen bonding to activated iodoarenes. Many of the activated bromoarene XB donors examined, however, were only marginally competitive with H_2O (and C–H) hydrogen bond donors for the chloride anions. A good example of this dichotomy is found through comparison of structures **7** and **8**. In the former, water solvates and ArI···Cl^- halogen bonding act in a complementary fashion to reinforce the observed crystalline supramolecular network, while in the latter charge-assisted halogen bonding is completely absent in favor of chloride–H-bonding contacts (despite similar degrees of solvation in the two structures). In the future, it will be interesting to examine the effect that

incorporation of H-bond donors into iodophenylpyridinium frameworks has on solid state interactions and halogen bonding. Based on the results of this study and the structure of 4-$IC_6H_4NH_3^+Cl^-$ reported previously by Rissanen and co-workers,[12b] halogen and hydrogen bonding to anionic XB acceptors may be capable of acting in concert to influence supramolecular assembly in a potentially predictable fashion.

A cationic pyridinium ring is also an integral feature of the crystallization substrates examined in this study. Indeed, the incorporation of this ring system provides a basis for enhanced halogen bond donor ability of the attached *N*-halophenyl groups via electron withdrawing inductive effects. These same inductive effects, however, also impart greater hydrogen bond donor ability upon the pyridinium C–H groups. In fact, pyridinium C–H···X^- hydrogen bonding is observed in each crystal structure. As discussed above, however, these hydrogen bonding interactions are compatible with ArI···X^- halogen bonding, but appear to occur in preference to (or at the expense of) ArBr···Cl^- halogen bonding in many cases. This may indicate that the H-bond donor ability of these C–H groups is equal to or surpasses the XB donor ability of the aryl bromines, but is less than the XB donor ability of the analogous iodoarenes. *N*-Haloarylpyridinium ring systems possess significant polarity as well, and one might imagine this feature could manifest itself through head-to-tail type π-stacking interactions. Significant π-π contacts were only observed in half of the structures examined (**1**-**2**, **4**, **6**, and **9**), and so it appears this non-covalent interaction is of generally lesser importance than solid state XB and H-bonding.

CONCLUSIONS

This study assessed the reliability of halogen bonding between *N*-haloarylpyridinium cations and halide anions in crystalline ion pair assemblies. Five pairs of iodo- and bromophenylpyridinium halides were prepared and structurally characterized. Examination of the resulting crystal structures reveals the universal occurrence of ArI···X^- (X = Cl or I) halogen bonding. In contrast, ArBr···Cl^- halogen bonding interactions in analogous substrates are not as frequent and are generally markedly weaker (according to distance criteria) than those encountered in the iodoarene series. We speculate that the differences observed in the two series of pyridinium salts are related to inherent differences in XB donor ability between the two halogens such that activated bromoarene XB donors are unable to effectively compete with hydrogen bond donors (water solvate molecules, aryl C–H groups) for the chloride anion acceptors. Halogen bonding of halide anions to similarly activated iodoarene residues under the same conditions, however, is not impeded. Examination of iodoarene substrates that possess XB donor:halide ion acceptor ratios of 2:1 illustrate the ability to generate extended halogen bonded networks and discrete halogen bonded dimers via Cl^- bridging interactions. The generation of these extended halogen bonding networks highlights the potential of diiodophenylpyridinium cations to exert structure-directing effects over solid state self-assembly processes. The identification of recurring XB motifs in additional substituted (polyiodo)phenylpyridinium salts is the subject of current studies.

ASSOCIATED CONTENT

Supporting Information

Crystallographic data in CIF format, additional figures, PXRD data, and tables of selected XB/HB distances and angles. This material is available free of charge via the Internet at http://pubs.acs.org.

AUTHOR INFORMATION

Corresponding Author

*Phone: 319-335-3805. Fax: 319-335-1270. Email: chris-pigge@uiowa.edu. Web: https://www.chem.uiowa.edu/pigge-group.

Notes

The authors declare no competing financial interest.

ACKNOWLEDGMENTS

We thank the Department of Chemistry, University of Iowa

REFERENCES

(1) a) Metrangolo, P.; Neukirch, H.; Pilati, T.; Resnati, G. *Acc. Chem. Res.* **2005**, *38*, 386-395. b) Metangolo, P.; Meyer, F.; Pilati, T.; Resnati, G.; Terraneo, G. *Angew. Chem. Int. Ed.* **2008**, *47*, 6114-6127. c) Rissanen, K. *CrystEngComm* **2008**, *10*, 1107-1113. d) Fourmigué, M. *Curr. Opin. Solid State Mater. Sci.* **2009**, *13*, 36-45. e) Troff, R. W.; Mäkelä, T.; Topić, F.; Valkonen, A.; Raatikainen, K.; Rissanen, K. *Eur. J. Org. Chem.* **2013**, 1617-1637.

(2) a) Metrangolo, P.; Resnati, G.; Pilati, T.; Liantonio, R.; Meyer, F. *J. Polym. Sci., Part A: Polym. Chem.* **2007**, *45*, 1-15. b) Fourmigué, M. *Struct. Bond.* **2008**, *126*, 181-207. c) Hanson, G. R.; Jensen, P.; McMurtrie, J.; Rintoul, L.; Micallef, A. S. *Chem. – Eur. J.* **2009**, *15*, 4156-4164. d) Bruce, D. W.; Metangolo, P.; Meyer, F.; Pilati, T.; Präsang, C.; Resnati, G.; Terraneo, G.; Wainwright, S. G.; Whitwood, A. C. *Chem. – Eur. J.* **2010**, *16*, 9511-9524. e) Bolton, O.; Lee, K.; Kim, H.-J.; Lin, K. Y.; Kim, J. *Nature Chem.* **2011**, *3*, 205-210. f) Cariati, E.; Cavallo,

G.; Forni, A.; Leem, G.; Metrangolo, P.; Meyer, F.; Pilati, T.; Resnati, G.; Righetto, S.; Terraneo, G.; Tordin, E. *Cryst. Growth Des.* **2011**, *11*, 5642-5648. g) Priimagi, A.; Cavello, G.; Forni, A.; Gorynsztejn-Leben, M.; Kaivola, M.; Metrangolo, P.; Milani, R.; Shishido, A.; Pilati, T.; Resnati, G.; Terraneo, G. *Adv. Funct. Mater.* **2012**, *22*, 2572-2579. h) Pang, X.; Zhao, X. R.; Wang, H.; Sun, H.-L.; Jin, W. J. *Cryst. Growth Des.* **2013**, *13*, 3739-3745. i) Priimagi, A.; Cavallo, G.; Metrangolo, P.; Resnati, G. *Acc. Chem. Res.* **2013**, *46*, 2686-2695. j) Meyer, F.; Dubois, P. *CrystEngComm* **2013**, *15*, 3058-3071.

(3) a) Mele, A.; Metrangolo, P.; Neukirch, H.; Pilati, T.; Resnati, G. *J. Am. Chem. Soc.* **2005**, *127*, 14972-14973. b) Metrangolo, P.; Carcenac, Y.; Lahtinen, M.; Pilati, T.; Rissanen, K.; Vij, A.; Resnati, G. *Science* **2009**, *323*, 1461-1464. c) Metrangolo, P.; Pilati, T.; Terraneo, G.; Biella, S.; Resnati, G. *CrystEngComm* **2009**, *11*, 1187-1196. d) Cavallo, G.; Metrangolo, P.; Pilati, T.; Resnati, G.; Sansotera, M.; Terraneo, G. *Chem. Soc. Rev.* **2010**, *39*, 3772-3783. e) Cametti, M.; Raatikainen, K.; Metrangolo, P.; Pilati, T.; Terraneo, G.; Resnati, G. *Org. Biomol. Chem.* **2012**, *10*, 1329-1333. f) Raatikainen, K.; Cavallo, G.; Metrangolo, P.; Resnati, G.; Rissanen, Terraneo, G. *Cryst. Growth Des.* **2013**, *13*, 871-877. g) Beyeh, N. K.; Cetina, M.; Rissanen, K. *Chem. Commun.* **2014**, *50*, 1959-1961. h) Zapata, F.; Caballero, A.; Molina, P.; Alkorta, I.; Elguero, J. *J. Org. Chem.* **2014**, *79*, 6959-6969. i) Massena, C. J.; Riel, A. M. S.; Neuhaus, G. F.; Decato, D. A.; Berryman, O. B. *Chem. Commun.* **2015**, *51*, 1417-1420. j) Lim, J. Y. C.; Beer, P. D. *Chem. Commun.* **2015**, *51*, 3686-3688.

(4) a) Kniep, F.; Walter, S. M.; Herdtweck, E.; Huber, S. M. *Chem. – Eur. J.* **2012**, *18*, 1306-1310. b) Jungbauer, S. H.; Schindler, S.; Kniep, F.; Walter, S. M.; Rout, L.; Huber, S. M. *Synlett*, **2013**, *24*, 2624-2628. c) Jungbauer, S. H.; Walter, S. M.; Schindler, S.; Rout, L.; Kniep, F.; Huber, S. M. *Chem. Commun.* **2014**, *50*, 6281-6284. d) He, W.; Ge, Y.-C.; Tan, C.-T. *Org.*

Lett. **2014**, *16*, 3244-3247. e) Takeda, Y.; Hisakuni, D.; Lin, C.-H.; Minakata, S. *Org. Lett.* **2015**, *17*, 318-321.

(5) a) Metrangolo, P.; Meyer, F.; Pilati, T.; Proserpio, D. M.; Resnati, G. *Chem. – Eur. J.* **2007**, *13*, 5765-5772. b) Pigge, F. C.; Vangala, V. R.; Kapadia, P. P.; Swenson, D. C.; Rath, N. P. *Chem. Commun.* **2008**, 4726-4728. c) Raatikainen, K.; Huuskonen, J.; Lahtinen, M.; Metrangolo, P.; Rissanen, K. *Chem. Commun.* **2009**, 2160-2162. d) Baldrighi, M.; Metrangolo, P.; Meyer, F.; Pilati, T.; Proserpio, D.; Resnati, G.; Terraneo, G. *J. Fluorine Chem.* **2010**, *131*, 1218-1224. e) Lieffrig, J.; Yamamoto, H. M.; Kusamoto, T.; Cui, H.; Jeannin, O.; Fourmigué, M.; Kato, R. *Cryst. Growth Des.* **2011**, *11*, 4267-4271. f) Kapadia, P. P.; Swenson, D. C.; Pigge, F. C. *Cryst. Growth Des.* **2011**, *11*, 698-706. g) Martí-Rujas, J.; Colombo, L.; Lü, J.; Dey, A.; Terraneo, G.; Metrangolo, P.; Pilati, T.; Resnati, G. *Chem. Commun.* **2012**, *48*, 8207-8209. h) Pigge, F. C.; Kapadia, P. P.; Swenson, D. C. *CrystEngComm* **2013**, *15*, 4386-4391. i) Lieffrig, J.; Jeannin, O.; Fourmigué, M. *J. Am. Chem. Soc.* **2013**, *135*, 6200-6210. j) Lieffrig, J.; Niassy, A. G.; Jeannin, O.; Fourmigué, M. *CrystEngComm* **2015**, *17*, 50-57.

(6) a) Brammer, L.; Espallargas, G. M.; Libri, S. *CrystEngComm* **2008**, *10*, 1712-1727. b) Bertani, R.; Sgarbossa, P.; Venzo, A.; Lelj, F.; Amati, M.; Resnati, G.; Pilati, T.; Metrangolo, P.; Terraneo, G. *Coord. Chem. Rev.* **2010**, *254*, 677-695. c) Ormond-Prout, J. E.; Smart, P.; Brammer, L. *Cryst. Growth Des.* **2012**, *12*, 205-216. d) Johnson, M. T.; Džolić, Z.; Cetina, M.; Wendt, O. F.; Öhrström, L.; Rissanen, K. *Cryst. Growth Des.* **2012**, *12*, 362-368. e) Smith, D. A.; Brammer, L.; Hunter, C. A.; Perutz, R. N. *J. Am. Chem. Soc.* **2014**, *136*, 1288-1291.

(7) a) Politzer, P.; Murray, J. S.; Clark, T. *Phys. Chem. Chem. Phys.* **2010**, *12*, 7748-7757. b) Legon, A. C. *Phys. Chem. Chem. Phys.* **2010**, *12*, 7736-7747. c) Politzer, P.; Murray, J. S. *ChemPhysChem* **2013**, *14*, 278-294.

(8) Murray, J. S.; Riley, K. E.; Politzer, P.; Clark, T. *Aust. J. Chem.* **2010**, *63*, 1598-1607.

(9) a) Beale, T. M.; Chudzinski, M. G.; Sarwar, M. G.; Taylor, M. S. *Chem. Soc. Rev.* **2013**, *42*, 1667-1680. b) Langton, M. J.; Robinson, S. W.; Marques, I.; Félix, V.; Beer, P. D. *Nature Chem.* **2014**, *6*, 1039-1043.

(10) Aakeröy, C. B.; Baldrighi, M.; Desper, J.; Metrangolo, P.; Resnati, G. *Chem. – Eur. J.* **2013**, *19*, 16240-16247.

(11) a) Freytag, M.; Jones, P. G.; Ahrens, B.; Fischer, A. K. *New J. Chem.* **1999**, *23*, 1137-1139. b) Logothetis, T. A.; Meyer, F.; Metrangolo, P.; Pilati, T.; Resnati, G. *New. J. Chem.* **2004**, *28*, 760-763. c) Awwadi, F. F.; Willett, R. D.; Peterson, K. A.; Twamley, B. *J. Phys. Chem. A* **2007**, *111*, 2319-2328. d) Awwadi, F. F.; Willett, R. D.; Twamley, B. *J. Mol. Struct.* **2009**, *918*, 116-122. e) Mukai, T.; Nishikawa, K. *Chem. Lett.* **2009**, *38*, 402-403. f) Caballero, A.; Zapata, F.; White, N. G.; Costa, P. J.; Félix, V.; Beer, P. D. *Angew. Chem. Int. Ed.* **2012**, *51*, 1876-1880. g) Zapata, F.; Caballero, A.; White, N. G.; Claridge, T. D. W.; Costa, P. J.; Félix, V.; Beer, P. D. *J. Am. Chem. Soc.* **2012**, *134*, 11533-11541. h) Gilday, L. C.; Lang, T.; Caballero, A.; Costa, P. J.; Félix, V.; Beer, P. D. *Angew. Chem. Int. Ed.* **2013**, *52*, 4356-4360. i) Walter, S. M.; Jungbauer, S. H.; Kniep, F.; Schindler, S.; Herdtweck, E.; Huber, S. M. *J. Fluorine Chem.* **2013**, *150*, 14-20. j) White, N. G.; Caballero, A.; Beer, P. D. *CrystEngComm* **2014**, *16*, 3722-3729.

(12) a) Gray, L.; Jones, P. G. *Z. Naturforsch.* **2002**, *57b*, 61-72. b) Raatikainen, K.; Cametti, M.; Rissanen, K. *Beilstein J. Org. Chem.* **2010**, *6*, No. 4.

(13) a) Garcia, M. D.; Blanco, V.; Platas-Iglesias, C.; Peinador, C.; Quintela, J. M. *Cryst. Growth Des.* **2009**, *9*, 5009-5013. b) Pignataro, L.; Papalia, T.; Slawin, A. M. Z.; Goldup, S. M. *Org. Lett.* **2009**, *11*, 1643-1646.

(14) a) Steinhardt, S. E.; Silverston, J. S.; Vanderwal, C. D. *J. Am. Chem. Soc.* **2008**, *130*, 7560-7561. b) Wang, M.; Han, R. H.; Han, X. *Anal. Chem.* **2013**, *85*, 9312-9320.

(15) a) Kost, A. N.; Gromov, S. P.; Sagitullin, R. S. *Tetrahedron* **1981**, *37*, 3423-3454. b) Yamaguchi, I.; Higashi, H.; Shigesue, S.; Shingai, S.; Sato, M. *Tetrahedron Lett.* **2007**, *48*, 7778-7781.

(16) Kassl, C. J.; Pigge, F. C. unpublished results.

(17) a) Raatikainen, K.; Rissanen, K. *Cryst. Growth Des.* **2010**, *10*, 3638-3646. b) Caballero, A.; Bennett, S.; Serpell, C. J.; Beer, P. D. *CrystEngComm* **2013**, *15*, 3076-3081. c) Sarwar, M. G.; Dragisić, B.; Dimitrijević, E.; Taylor, M. S. *Chem. – Eur. J.* **2013**, *19*, 2050-2058.

(18) Bondi, A. *J. Phys. Chem.* **1964**, *68*, 441-451.

(19) Attempts to grow bulk crystalline samples of **1**·$(H_2O)_2$ were not successful. Instead, a monohydrate of 4-iodophenylpyridinium chloride was obtained and characterized by single crystal and powder XRD (CCDC # 1405250). The mono- and di-hydrates of **1** display similar features in the extended packing. Details are included in the supporting information.

(20) See reference 17b for a similar observation.

(21) Crystals of **5** proved to be fragile and a bulk sample suitable for PXRD analysis could not be obtained.

(22) Very few other examples of halide ion-bridged dimerization of 1,3-dihaloarenes have been reported: a) Yamamoto, H. M.; Kato, R. *Chem. Lett.* **2000**, 970-971. b) Metrangolo, P.; Meyer, F.; Pilati, T.; Resnati, G.; Terraneo, G. *Chem. Commun.* **2008**, 1635-1637. c) Tiguero, S.; Llusar, R.; Polo, V.; Fourmigué, M. *Cryst. Growth Des.* **2008**, *8*, 2241-2247.

(23) Aakeröy, C. B.; Chopade, P. D.; Desper, J. *Cryst. Growth Des.* **2013**, *13*, 4145-4150.

For Table of Contents Use:

The propensity of crystalline mono- and di-halophenylpyridinium cations (halogen = Br or I) to engage in solid-state charge-assisted halogen bonding with chloride anions was examined.

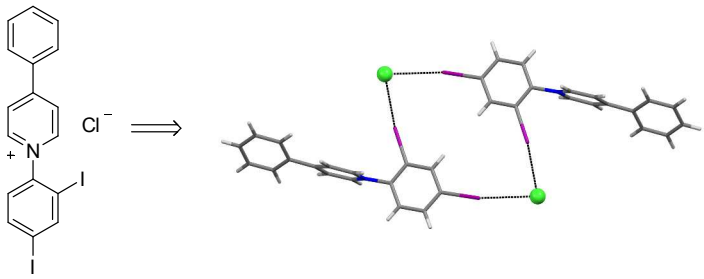

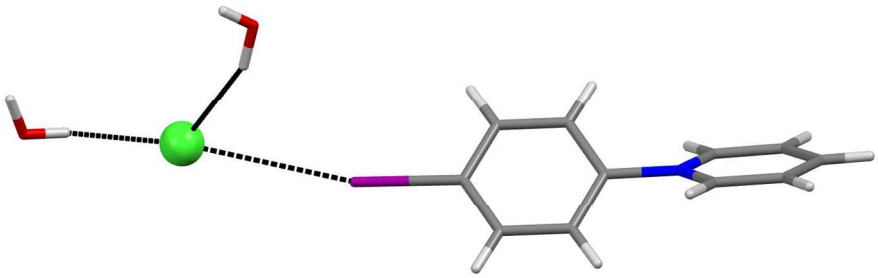

Asymmetric unit in 1. Chloride anion shown as green sphere. I···Cl– d = 3.436 Å, C–I···Cl– = 166.27º.
450x237mm (96 x 96 DPI)

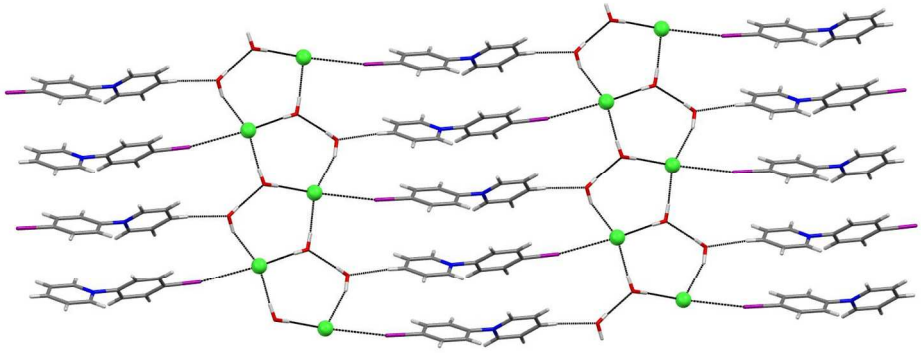

Interplay of XB and chloride ion solvation in 1.
450x237mm (96 x 96 DPI)

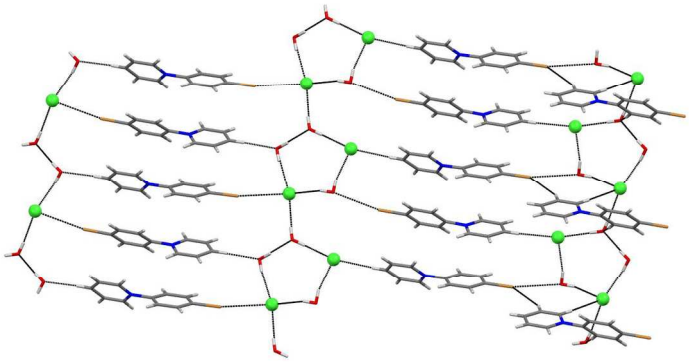

Halogen and hydrogen bonding interactions in 2. See text for XB and HB metrics.
506x194mm (96 x 96 DPI)

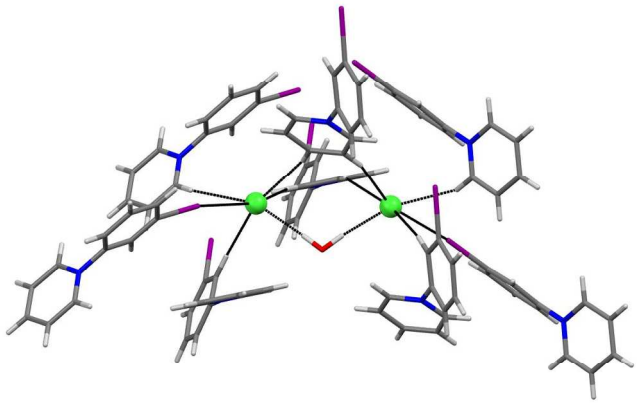

Intermolecular interactions of chloride ions in 3.
506x237mm (96 x 96 DPI)

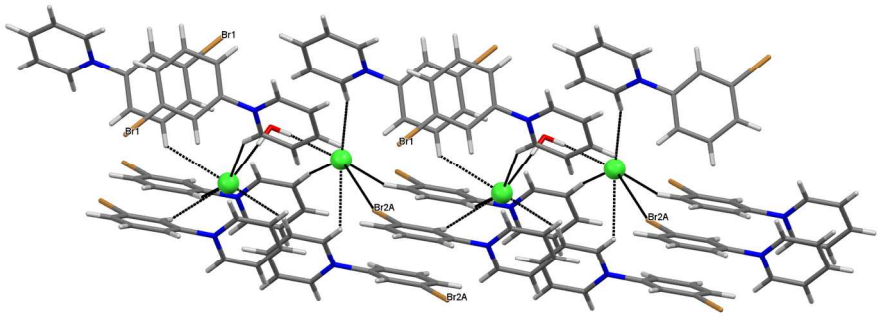

Coordination environment of chloride ions in 4.
506x194mm (96 x 96 DPI)

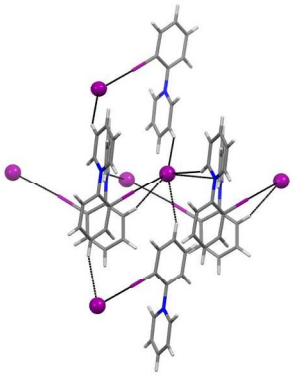

ArI···I− halogen bonding and the coordination sphere around iodide in 5 (iodide anions shown as purple spheres).
506x194mm (96 x 96 DPI)

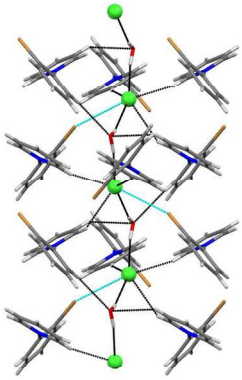

Non-covalent interactions surrounding the chloride ion in 6. "Halogen bond" indicated in light blue is equal to the sum of the Br···Cl− vdW radii.
506x237mm (96 x 96 DPI)

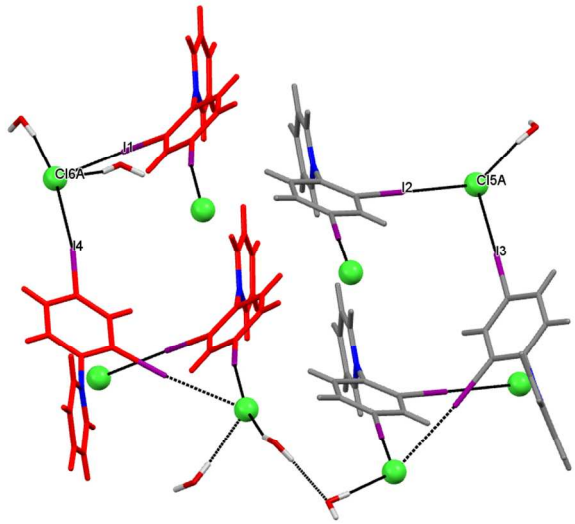

Extended halogen bonding networks in helical assemblies found in 7. Helices derived from unique diiodophenylpyridinium cations are color coded red and grey. Halogen bonding metrics: I1···Cl6A− = 3.140 Å (17% < ΣvdW), I4···Cl6A− = 3.563 Å (6% < ΣvdW), C–I1–Cl6A− = 173.69º, C–I4–Cl6A− = 172.06º, I2···Cl5A− = 3.230 Å (15% < ΣvdW), I3···Cl5A− = 3.318 Å (12% < ΣvdW), C–I2–Cl5A− = 176.37º, C–I3–Cl5A− = 177.22º.
337x190mm (96 x 96 DPI)

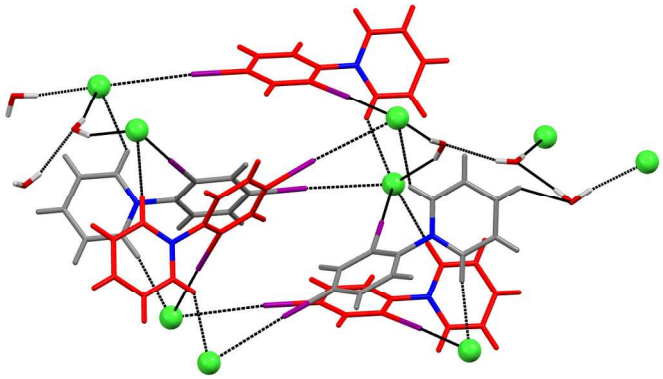

Bridging of unique helices in 7 through chloride ions by water solvates and C–H···Cl– hydrogen bonding.
506x194mm (96 x 96 DPI)

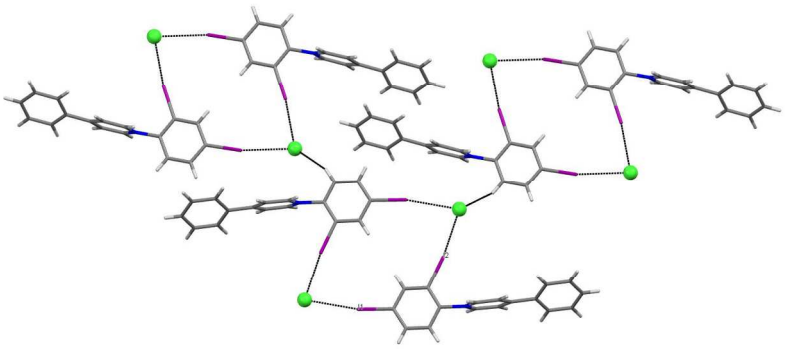

Halogen bonded macrocyclic dimers observed in 9. See text for XB metrics.
506x194mm (96 x 96 DPI)

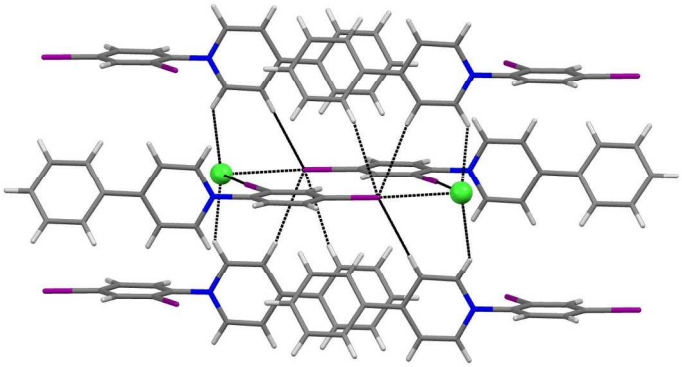

Stacking of layers shown in Figure 10 in an ABA fashion.
506x194mm (96 x 96 DPI)

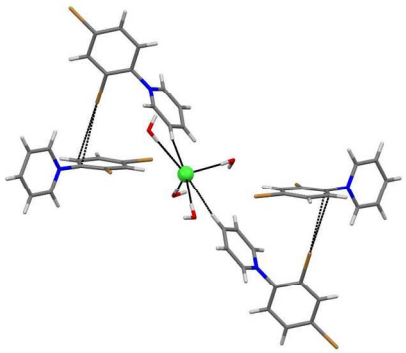

Environment around chloride ions in 8 and the absence of Br···Cl– halogen bonds.
506x194mm (96 x 96 DPI)

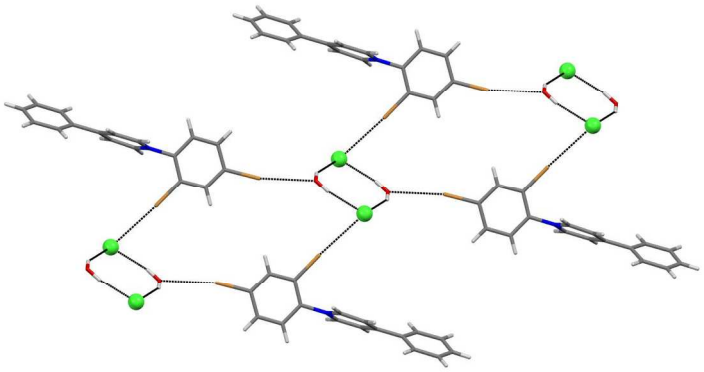

Principal hydrogen/halogen bonding network in 10.
506x194mm (96 x 96 DPI)

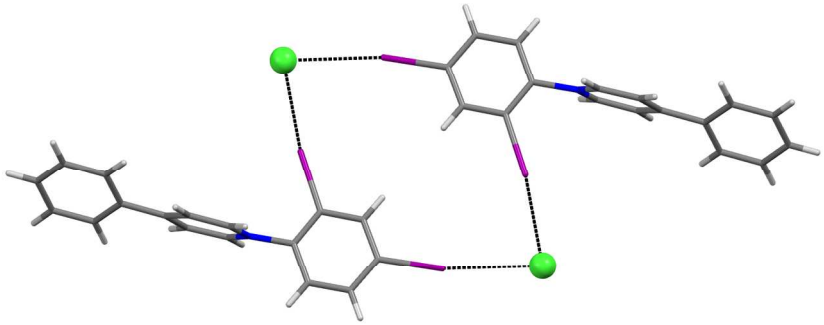

506x194mm (96 x 96 DPI)